

DAMAGE TOLERANCE IMPROVEMENT OF LASER BEAM WELDED FUSELAGE STRUCTURES VIA CRENELLATIONS

J. Lu *, N. Kashaev, N. Huber

Institute of Materials Research, Materials Mechanics, Helmholtz-Zentrum Geesthacht

Keywords: *crenellation, damage tolerance, biaxial fatigue test, kinked cracks*

Abstract

In this work the concept of the crenellation for improving the fatigue resistance of the fuselage skin by systematic thickness variations was examined under the service-related biaxial loading condition. Fatigue tests imitating the long-term cyclic load due to the repetitive fuselage pressurizations were carried out on both crenellated and flat panels with straight and kinked cracks. An unexpected high propagation rate of the kinked crack in the crenellated specimen was found, which reduced the fatigue life even compared to the uncrenellated specimens. FEM models validated by experiments were applied to understand the corresponding fatigue behavior. The observed high crack propagation rate was found correlated with the mode III load and a possible change in mode I crack closure behavior. The source of the mode III load was analyzed based on FEM simulation, which was found to be coupled with the biaxial loading condition.

1 Introduction

Laser beam welding (LBW) is a high efficient joining technique for fuselage construction. A complete replacement of conventional riveting with LBW is expected to bring a 15% reduction in construction cost [1]. However, LBW leads to a monolithic integral structure which shows inferior damage tolerance compared to the conventional riveted structures [2]. Before LBW is widely applied in the fuselage construction,

significant improvement in terms of fatigue resistance and residual strength of the welded structure must be achieved.

The concept of the crenellation is aimed to enhance the fatigue performance of laser beam welded stringer-stiffened fuselage panels [3]. As shown in Fig. 1, the thickness of the fuselage skin is purposely increased and decreased in selected regions, the weights of which balance each other. The fatigue life gain in the thick region outweighs the fatigue life shortening in the thin regions, which leads to an overall improvement of fatigue life. Uz et al. [3] showed under uniaxial loading conditions that well designed crenellations can achieve over 65% increase of fatigue life in stringer-stiffened panels with a straight crack propagating perpendicular to the crenellation direction.

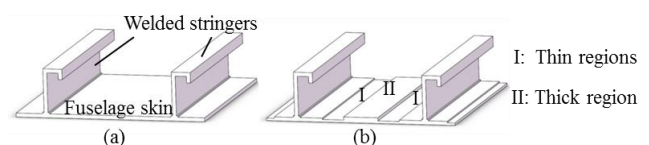


Figure 1 – (a) flat and (b) crenellated structure with the same weight

However, the performance of crenellations with regard to the service-related biaxial loading case was yet unknown. In addition the assumed straight fatigue crack path in Uz's work is an idealized case. In practice fatigue crack deflections are often observed in pressurized fuselage panels [4]. Deflected fatigue cracks, which normally grow under mixed mode load, behave quite differently from the straight cracks in the aspect of an altered crack closure level.

Borrego et al. [5] observed a strong increase of the crack opening load ($P_{op,I}$) with a decreased length of the kinked crack in the single edge notched specimens (SENT). The authors consider that the roughness induced crack closure (RICC) introduced by the asperity contact of crack faces under mixed load should be responsible for this increase of $P_{op,I}$. Qian and Fatemi [6] observed a relative lower fatigue crack growth (FCG) rates of deflected cracks compared to the straight cracks, when the FCG rates are plotted against the corresponding stress intensity factor ranges calculated by FEM simulation. This indirectly reflects the relatively higher $P_{op,I}$ of deflected cracks. However, in the simulation work of Kibey et al. [7] $P_{op,I}$ was observed to firstly decrease after the crack deflection, which then, as the crack extends, steadily increases towards the $P_{op,I}$ of pure mode I cracks. This contradiction probably originates from the fact that in the simulation the microscopic zigzag of crack path was neglected, which leads to a significant underestimation of the RICC due to the shear slip of crack faces. Those previously mentioned studies were based on flat specimens. The thickness variations in crenellated structures could possibly further tune the crack closure level of deflected cracks, which needs further investigation.

In this work the fatigue behavior of crenellated panels with both straight and kinked cracks were investigated under service-related biaxial loading scenario. This loading scenario is aimed at imitating the repetitive fuselage load from the cabin pressurization and depressurization throughout thousands of flights, which is one of the major concerns for the multiple site damage in the fuselage [8]. FE analysis was carried out in conjunction with experiments to achieve a deep understanding of the corresponding fatigue behavior.

2 Materials and Method

2.1 Geometries of the Crenellation Pattern

The crenellation pattern investigated in this study is equivalent in weight to a reference

sheet with a thickness of 2.9 mm, the detailed geometry of which is shown in Fig. 2. In each bay a centered thickened region with a thickness of 4.1mm was designed for crack retardation. The extra weight of this pad-up is compensated by two thickness reduction regions (1.9mm) located on both sides. In order to focus on the effect of crenellation itself, stringers were not welded for the present step of study.

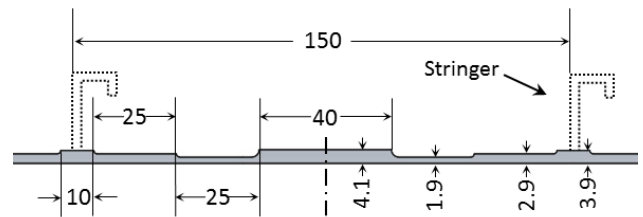


Figure 2 - Geometries of a crenellated sheet with welded stringers (unit: mm)

2.2 Specimens and Experimental Setup

The specimens for biaxial fatigue testing are 560 mm × 560 mm square panels machined from a 4.5 mm thick AA2139 sheet after T351 heat treatment (Fig.3b). The outer region of the specimens retains the original thickness of the sheet. Four rows of 16 bolt holes were drilled along each rim of the specimens for fixation. In the center part of specimens (400 mm × 400 mm square region) the thickness was either reduced symmetrically from both sides to 2.9mm in the reference panels or from one side to the corresponding dimension of crenellations in the crenellated panels. The size of the specimens allows the placement of two bays of crenellation patterns. The welding sites of stringers depicted in Fig. 2 were positioned at the red lines as shown in Fig. 3b. A pre-crack was introduced into the specimens as shown in the inset of Fig. 3b. A hole with diameter of 1mm was firstly drilled at the panel center. Then a 12mm long and 0.6mm wide notch was made by electro discharge machining, which was symmetric to the center hole. Before subsequent fatigue tests strain gauges were applied on the specimens' surface.

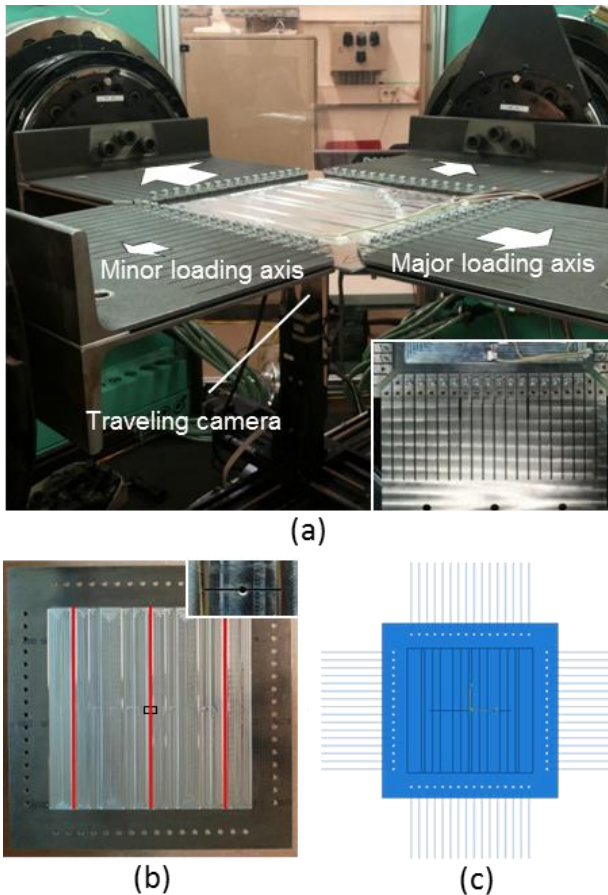


Figure 3 – (a) experimental setup, (b) specimen and (c) corresponding FEM model

The specimens were tested with a biaxial servo-hydraulic testing machine (Fig. 3a), each load axis of which has a capacity of 1000kN. The specimens were fixed in the horizontal plane by specially designed clamping devices (Fig. 3b), which can ensure a homogeneous stress distribution in the center part of specimens. Constant amplitude cyclic loading in both axes was applied to the specimens in pace with R ratio of 0.1. The maximum load in the major loading was 112.4kN while that in the minor loading direction was 56.2kN. At the maximum load the nominal stress in the major loading direction was about 90MPa, which corresponds to the stress level of the hoop pressure inside the fuselage skin due to cabin pressurization. The minor load corresponds to the axial pressure of the fuselage skin in the flight state. During tests the positions of both crack tips were recorded at about every 1 mm of crack growth by a traveling camera underneath the specimens with an accuracy of 0.01mm. The fatigue crack propagation rate was obtained by

the secondary polynomial fitting of 5 consecutive measurement points according to ASTM E647 [9].

2.3 FEM Modeling Approach

FEM models for the experimental setup of the fatigue tests (Fig. 3c) were established using the commercial code ABAQUS (version 6.12). Quadrilateral 4-node shell elements with reduced integration were applied to model the panels of specimens. The clamping device was modeled as a series of beams using quadratic 3-node beam elements. One end of each beam was tied to the corresponding bolt hole in the specimen panel with untied rotation degrees of freedom. The other ends of the four groups of beams were kinetically coupled to four controlling points respectively, on which the maximum loads in a load cycle were applied. The clamping devices modeled were only allowed to move in the direction of respective loading axes with all other displacement and rotation degrees of freedom constrained. The mesh size along the crack path was refined to 1 mm × 1 mm. The propagation of the crack was realized by consecutively releasing the tied duplicate node pairs on the crack line. The stress intensity factor (SIF) profile along the crack path was obtained through the calculation of the strain energy releasing rate (SERR) using a two-step crack closure technique as described by Kruegel[10].

3 Results and Discussion

3.1 Biaxial Fatigue Tests

The specimens tested are listed in Table 1. To investigate the behavior of deflected cracks, different types of center notches for crack initiation were made in two groups of crenellated and flat specimens. The notches of the first group (specimen 1, 2) were perpendicular to the major loading direction while those of the second group (specimen 3, 4) were 45° inclined. During the fatigue tests, the cracks always propagated perpendicular to the major loading direction, which brought straight cracks in the first case and kinked cracks with a

deflection angle of 45° in the latter case. The fatigue lives of tested specimens are shown in Fig. 4.

Table 1 – list of specimens

specimens	crenellation	thickness	inclination of initial notch
1	no	2.9mm	0°
2	yes	~2.9mm	0°
3	no	2.9mm	45°
4	yes	~2.9mm	45°

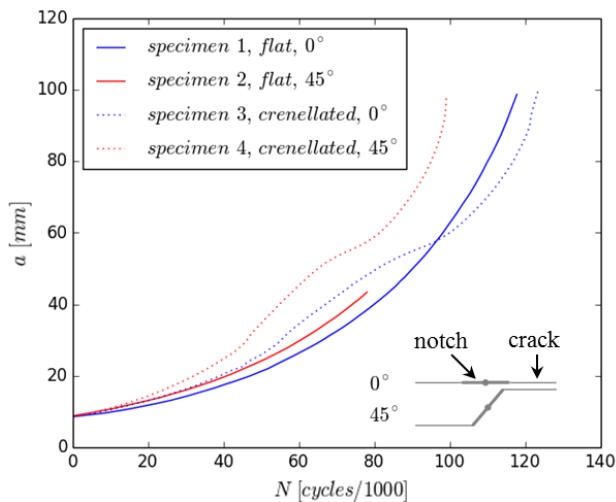


Figure 4 – Fatigue lives of tested specimens

As for the straight cracks, it is shown that crenellations slightly improved the fatigue life of the panel in non-stiffened state by about 7%. The value is very close to the fatigue life gain (around 9%) under uniaxial loading condition as found by Uz [11], which indicates a negligible influence of the load biaxiality with respect to the performance of crenellations.

In the group of flat specimens, the kinked crack propagates slightly faster than the straight crack. However, in the group of crenellated specimens the acceleration of propagation of the kinked crack is much more pronounced. The kinked crack in the crenellated specimen grows even faster than the flat specimens. Thus, the introduction of crenellations would not always improve the fatigue performance. This information is important for deciding the application region of crenellations in fuselage. In most parts of the fuselage skin, the loading state of material is dominated by the hoop pressure caused by fuselage pressurization. Fatigue cracks are expected to initiate and grow

straightly in the direction along the fuselage axis [12]. In such situation crenellations can be safely applied. However in the side regions near wing attachment, significant shear load exists [13], which could possibly deviate the crack from its original path. A similar accelerated fatigue crack growth could occur as observed in the experiment and this would put the application of crenellations into risk.

3.2 FEM Modeling of Biaxial Fatigue Tests

Although plastic deformation occurred surrounding the crack tips in the fatigue tests, the FEM models for stress intensity factor extraction were based on pure elasticity. The size of plastic zones (r_p) in the beginning and at the end of the fatigue tests of flat specimens are estimated (Table 2) by the equation according to Anderson [14]:

$$r_p = \frac{1}{\pi} \left(\frac{K_I}{\sigma_{YS}} \right)^2 \quad (1)$$

where σ_{YS} is the yield strength of the material, and K_I is the mode I stress intensity factor. As shown in Table 2 the plastic zone sizes developed at crack tips are far smaller than the corresponding crack lengths. Thus the small scale yielding condition is valid in our tests. The fatigue behaviors of tested specimens are considered to be dominated by the elastic response of the cracked structure, and the crack tip conditions can be uniquely characterized by stress intensity factor extracted from the FEM models based on pure elasticity.

Table 2 – estimated plastic zone size with different crack lengths in flat specimens

Half rack length	Plastic zone size
7mm	80μm
100mm	1.18mm

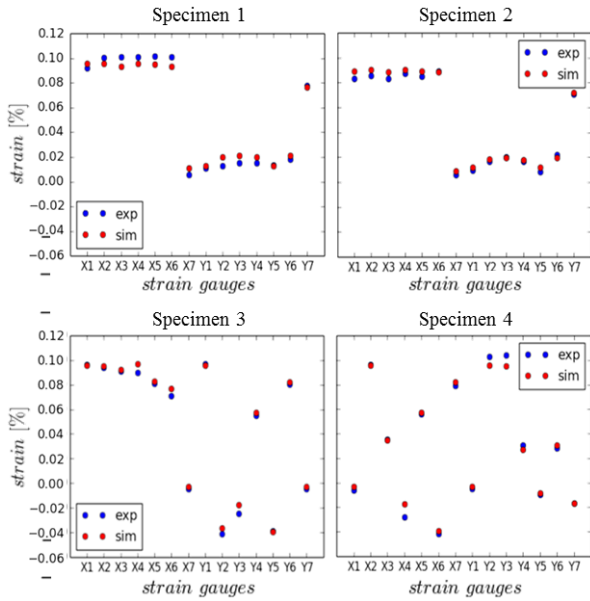


Figure 5 – Comparison of measured (*exp*) and predicted (*sim*) strain values at maximum load during a load cycle

The FEM models were firstly examined in terms of correctly characterizing the elastic deformation of the specimens. This was ensured by a good agreement (the deviations are mostly within 5%) between the strain measurements via the applied strain gauges in experiments and the strain values extracted from the corresponding locations in FEM models in simulations (Fig. 5). The slight systematic deviation in Specimen 1 is due to the small curvature introduced during the machining of the panel, which was not considered in the simulation.

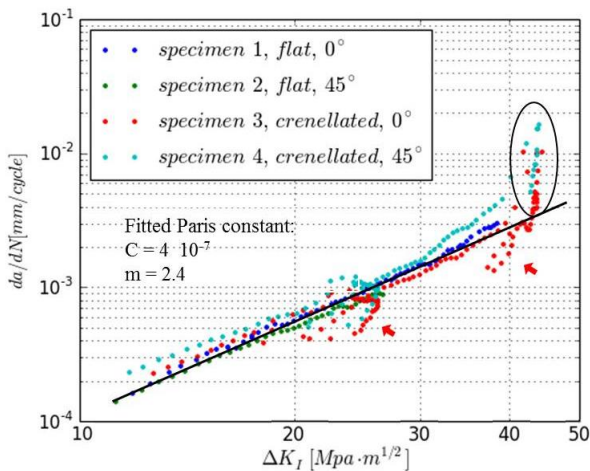


Figure 6 – da/dN - ΔK_I plot of the four specimens

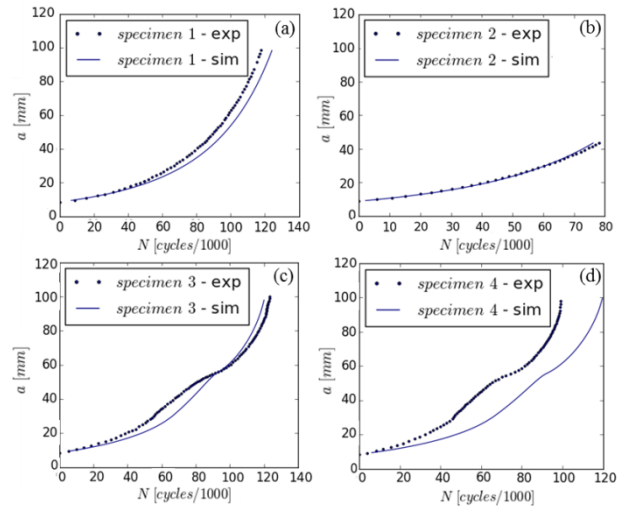


Figure 7 – Experimentally measured (*exp*) and predicted (*sim*) fatigue life based on Paris Law and fitted Paris constants

Then the FEM models were further validated based on a cross-validation between the specimens with different geometries and crack shapes. The experimentally measured fatigue crack propagation rates (da/dN) were plotted against the corresponding mode I stress intensity factor ranges ΔK_I extracted from simulation as shown in Fig. 6. The data points of the first three specimens fall into the same narrow scatter band with a linear trend as dictated by Paris Law:

$$\frac{da}{dN} = C \cdot \Delta K_I^m \quad (2)$$

The Paris constants C and m were obtained through a linear fitting as shown by the black line. When ΔK_I becomes very large, the corresponding da/dN values tend to deviate from this black line (marked by the black circle) due to the occurrence of stage III fatigue growth, which cannot be described by Paris Law. Since the models are based on pure elasticity, any change of crack closure behavior, which is normally related of the change of crack tip deformation, can be clearly reflected in Fig. 6. According to Uz the peaked ΔK_I profile at the thickness steps of crenellations leads to overloading-like load history effects as shown by the red arrows. This occurred 2 times in each of our crenellated specimens at the half crack length of 30 and 95mm respectively.

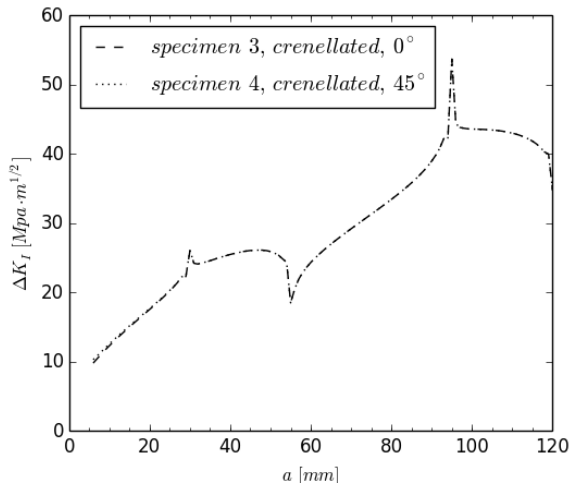


Figure 8 – ΔK_I profiles of straight and deflected cracks in crenellated specimens

The above mentioned deviations from Paris Law are rather localized and the overall fatigue life of first three specimens can still be predicted by our FEM models with good accuracy as shown in Fig. 7a, b, c. In principle the same validated simulation procedure should also work for specimen 4. However, the fatigue life was considerably overestimated by the calculation based on ΔK_I (Fig. 7d). Note from Fig. 8 that although the kinked crack propagated much faster than the straight crack in crenellated panels, the corresponding ΔK_I profiles for both cases are nearly identical. It indicates the driving force of both cases for the mode I crack should be the same. This unexpected high crack growth rate probably arises out of the shear mode loads, which were not considered in the previous prediction step based on ΔK_I .

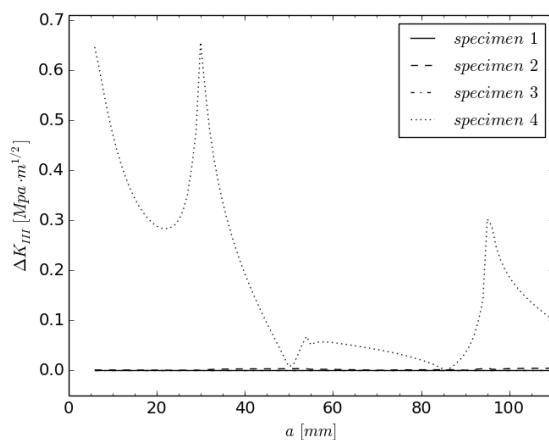


Figure 9: ΔK_{III} profile of the specimens

As shown in Fig. 9, only in specimen 4 the anti-plane shear (mode III) load was found. The

magnitude of ΔK_{III} along crack path is approximately in accordance with the corresponding increase of da/dN with respect to the expected ones located on the black line in Fig. 6. As shown in Fig. 9, in the first 50mm of fatigue crack growth the ΔK_{III} decreases from around 0.6 MPa·m^{1/2} to nearly zero. The same trend was also found in the deviation of the measured da/dN from the common scatter band in Fig. 6, which nearly diminishes after the first load-history effect region of crenellations (left red arrow, corresponding half crack length range: 30-45 mm). When the half crack length is over 90mm, considerable mode III load occurs again. Accordingly a large deviation of da/dN values in Fig. 6 was found around the second load-history effect region (right red arrow, starting from the half crack length of 95mm). This high accordance implies a direct correlation between the unexpected high crack growth rate in specimen 4 and the presence of mode III load.

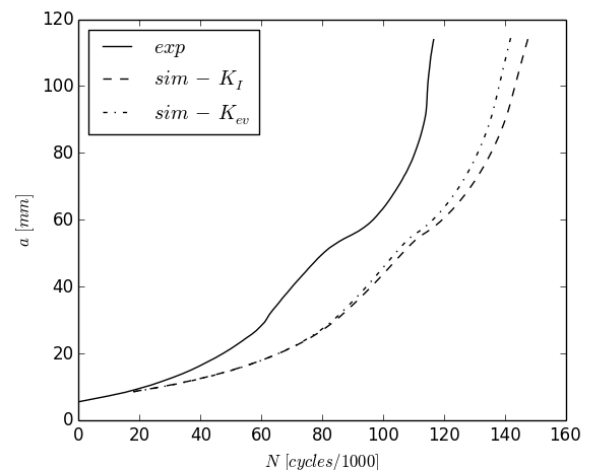


Figure 10 – Experimentally measured fatigue life of the specimen 4 (exp) and the predicted fatigue lives based K_I (sim- K_I) and K_{III} (sim- K_{III})

The contribution of the mode III load to the accelerated FCG rate can be attributed to either providing extra energy for FCG directly or indirectly influencing the driving force via the mode I crack opening level. As shown in Fig. 8 and Fig. 9 the magnitude of mode III load is actually trifling compared to Mode I load in terms of stress intensity factor. Even if the equivalent stress intensity factor is applied according to Tanaka [15]:.

$$\Delta K_{ev} = [\Delta K_I^4 + 8\nu\Delta K_{III}^4]^{0.25} \quad (3)$$

which takes into account the driving force contribution from mode III load, there is still a significant discrepancy between the predicted and experimentally observed fatigue life as shown in Fig. 10.

Therefore the additional driving force for the unexpectedly high da/dN values in specimen 4 should come from a reduced mode I crack opening level and an increased effective range of ΔK_I . As aforementioned in the simulation of Kibey et al. [7] a decrease of mode I crack opening load was observed after the crack deflection, which was found related with the in-plane shear (mode II) load. It is possible that the anti-plane shear (mode III) load in specimen 4 also leads to such a reduction in mode I crack opening level. However, the in-plane shear movement of crack faces is also accompanied by significant RICC mainly due to the asperity contact along the microscopically zigzag crack path, which outweighs this crack closure reduction effect. Thus in experiments of some previous researchers a higher crack opening level was actually observed [5,6]. For the anti-plane displacement caused by mode III load, the movement of crack faces is perpendicular to the crack line, the tortuosity of the crack path would not result in significant interference of crack faces in this mode of displacement. Thus only the crack closure reduction effect was observed in specimen 4.

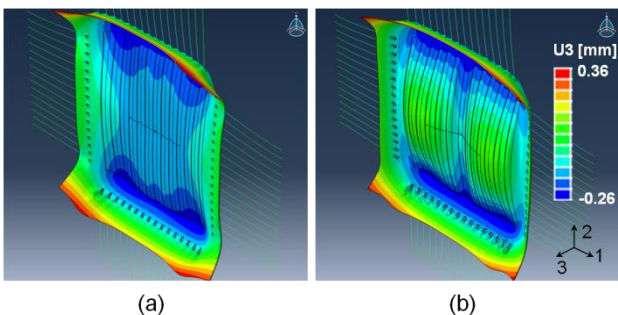


Figure 11 – Out of plane bending of crenellated specimens under biaxial loads (a) biaxial load ratio 0.1 (b) biaxial load ratio 0.5

The deflected cracks investigated in our specimens break the symmetry of the part with respect to crack line, which introduce the

different displacements between the upper and lower crack mouth and thus result in the relative shear movement at the crack tip. The mode III shear movement is actually a product of the broken symmetry and the out of plane bending of crenellated panels due to the reduced stiffness on the crenellated side in a direction transverse the crenellation. This out of plane bending only become pronounced with increasing biaxiality of external load as shown in Fig. 11. Since biaxial loading is the most common situation in fuselage material, the influence of deflected cracks must be considered to make a reasonable fatigue life assessment of crenellated structures for airframe application.

4 Conclusion

The fatigue performance of both flat and crenellated specimens was examined under biaxial loading conditions. It was found that the load biaxiality has no obvious effect on the fatigue life improvement in crenellated panels with straight cracks compared to the uniaxial loading case. Under biaxial loading condition a deterioration of fatigue resistance was found in the crenellated specimen with a kinked crack. The observed increase of the crack propagation rate was found to be correlated with the mode III load. The additional driving force for the crack propagation should come from the reduced mode I crack opening level, which is probably caused by the presence of mode III load.

Acknowledgement

The authors would like to thank Mr. Jürgen Knaack, Mr. Kay Erdman, Mr. Balzereit and Mr. Jie Liu from the department of Material Mechanics of Helmholtz Zentrum Geesthacht for their support in the experimental work and during the writing of the paper.

References

- [1] Rötzer I. Laser-beam welding makes aircraft lighter. *Fraunhofer Magazine*, No. 1, pp 36-37, 2005.
- [2] Palm F. Can welded fuselage structures fulfil future A/C damage tolerance requirements? *First International Conference on Damage Tolerance of Aircraft Structures*, Delft, 2007.
- [3] Uz M -V, Koçak M, Lemaitre F, Ehrström J –C, Kempa S and Bron F. Improvement of damage tolerance of laser beam welded stiffened panels for airframes via local engineering. *International Journal of Fatigue*, Vol. 31, pp 916-926, 2007.
- [4] Pettit R G. *Crack turning in integrally stiffened aircraft structures*. Doctor thesis, Cornell University, 2000
- [5] Borrego L P, Antunes F V, Costa J M and Ferreira J M. Mixed-mode fatigue crack growth behavior in aluminum alloy. *International Journal of Fatigue*, Vol. 28, pp 618-626, 2005.
- [6] Qian J and Fatemi A, Fatigue crack growth under mixed mode I and II loading. *Fatigue & Fracture of Engineering Materials & Structures*, Vol. 19, No. 10, pp 1277-1284, 1996.
- [7] Kibey S, Sehitoglu H and Pecknold D A, Modeling of fatigue crack closure in inclined and deflected cracks. *International Journal of Fracture*, Vol. 129, pp 279-308, 2004.
- [8] Wang L, Chow WT, Kawai H and Atluri S N. Predictions of widespread fatigue damage thresholds in aging aircraft. *AAIA Journal*, Vol. 36, No. 3, pp 457-464, 1998.
- [9] ASTM E647 Standard test method for measurement of fatigue crack growth rates.
- [10] Krueger R. Virtual crack closure technique: History, approach, and applications. *Applied Mechanics Reviews*, Vol. 57, No. 2, pp 109-143, 2004.
- [11] Uz M –V. *Improvement of damage tolerance of laser beam welded aerospace structures via local engineering*. Doctor thesis, Technical University Hamburg-Harburg, 2010.
- [12] Goranson U G. Damage tolerance – facts and fiction. *First International Conference on Damage Tolerance of Aircraft Structures – Keynote Presentation*, Delft, 2007.
- [13] Suresh S. *Fatigue of Materials*. 2nd edition, Cambridge University Press, 2003.
- [14] Anderson T L. *Fracture Mechanics*. 3rd edition, Taylor & Francis, 2011.
- [15] Tanaka K. Fatigue crack propagation from a crack inclined to the cyclic tensile axis. *Engineering Fracture Mechanics*, Vol. 6, pp 493-507, 1974.

Contact Author Email Address

jin.lu@hzg.de

Copyright Statement

The authors confirm that they, and/or their company or organization, hold copyright on all of the original material included in this paper. The authors also confirm that they have obtained permission, from the copyright holder of any third party material included in this paper, to publish it as part of their paper. The authors confirm that they give permission, or have obtained permission from the copyright holder of this paper, for the publication and distribution of this paper as part of the ICAS 2014 proceedings or as individual off-prints from the proceedings.